Institute of Paper Science and Technology
Atlanta, Georgia

IPST TECHNICAL PAPER SERIES

NUMBER 425

MODELING A CORRUGATING MEDIUM PAPERMACHINE FOR IMPROVED EDGEWISE COMPRESSIVE STRENGTH

G.L. JONES

FEBRUARY 1992

Modeling a Corrugating Medium Papermachine for Improved Edgewise Compressive Strength

G.L. Jones

Submitted to
TAPPI Papermakers Conference
April 5–8, 1992
Nashville, TN

Modeling a Corrugating Medium Papermachine for Improved Edgewise Compressive Strength

GARY L. JONES

The Institute of Paper Science and Technology
Atlanta, Georgia

ABSTRACT

The MAPPS simulation system was used to develop a detailed model of a corrugating papermachine to predict tensile and compressive properties with varying papermaking conditions such as OCC content, refiner load, pressing pressure, machine speed and calender loading. The model system was validated through statistical comparisons with machine paper and handsheet data from a three-day mill trial. Unexpectedly, both standard statistical methods and the simulation models showed that refining and wet pressing had only subtle effects on compressive strength while increasing OCC content actually improved tensile and compressive properties. Machine speed had little if any effect over a wide range. Increasing calendering load increased density and elastic moduli substantially but had only a small negative effect on specific modulus and compressive strength.

KEY WORDS: Corrugating medium, elastic properties, process simulation, papermachine models, paper strength, performance attributes.

PERFORMANCE ATTRIBUTES

A novel system of Performance Attribute (PAT) models were integrated with existing and/or new mass and energy balance models in MAPPS (Modular Analysis of Pulp and Paper Systems) to predict both handsheet and machine-paper properties for a range of grades formed with a variety of pulps of varying pulping and species. A machine trial was designed to validate the PAT system for corrugating medium.

The concept of end-use performance modelling is based on new a class of non-conservative variables (PAT's) representing many basic properties of fibers and the fiber network. The PAT modeling system is used to quantify the interactions between fibers and the fiber network, processing conditions, and end-use performance characteristics, to provide a new approach to solve product quality problems.

Performance attributes are composed of a set of 29 variables which describe the state of the fiber furnish or the fiber network at each point in the papermaking process. PAT values are initialized by fiber species and suspended solids data bases. PAT models predict the change in PAT's for each pulping or papermaking operation. Handsheet or machine paper properties can be determined for any stream by paper property models based on local performance attributes. With this system it is possible to calculate product quality development from the wood yard to the reel.

PAT's can be classified as component (i.e., fiber or filler) attributes or network attributes. Fiber or filler attributes include composition, shape, surface area, physical and optical properties. Network PAT's include contact area, bond area, and anisotropy. Anisotropy, in turn, includes factors such as sidedness, formation, fiber orientation and stress distribution variables. Each of these variables may be affected differently by each pulp and paper unit operation.

Previous studies showed that the model predictions were reasonable and consistent for newsprint and mechanical pulping (Jones 1988, 1989, 1990). However, these studies did not deal with issues such as variability, trends and process sensitivity. A two-part machine trial was designed to consider these issues and to determine sensitivity of corrugating medium tensile and compressive properties to important independent variables such as OCC content, refining load, press load and calender load. The trial was conducted on the corrugating medium paper machine at MacMillan Bloedel, Pine Hill, Alabama.

PROPERTY MODEL VALIDATION

Validation is defined as "reasonable" agreement between measurements and predictions, taking into account measurement error and other sources of variation such as CD variability. The validation was limited to the paper machine area beginning at the high density tanks and including the major paper machine operations such as stock preparation, sheet forming, white water recovery, wet pressing, drying and converting. Although CD variations were expected for some properties, the model is restricted to predictions of an MD profile.

Comparisons between measurements and predictions are based on handsheet and machine paper properties. Handsheets were made from composite pulps collected at five locations in the paper machine area. Validation criteria are based on statistical measures of "goodness of fit" and estimates of factors contributing to variability such as measurement error, errors in estimating process conditions and transient effects. Predictions which fell within the confidence band around the mean measurements indicate a valid model. The band includes the average measurement error plus CD variability and errors associated with uncertainty in input data.

PROCESS VARIABLES

Primary test variables summarized in Table 1 were weight fraction OCC, semi-chem (hole) refiner and tickler refiner specific speed, third nip press load and calender stack load. One other important uncontrolled variable was semi-chem high density CSF. The original intent was to change each variable separately and to achieve a "steady state" between each change. In practice, several variables (both controlled and uncontrolled) changed simultaneously, and the results show the superposition of several variables.

PROCESS MODEL

There are a number of novel aspects to the corrugating medium process model. The high density storage tanks were represented by stream initialization blocks which initialized both the material/energy and the performance attributes of the virgin semi-chem and OCC furnishes. Because the OCC is a mixture of hardwood and softwood components, two blocks (one for the softwood and one for the hardwood components of the OCC) were used. The characteristics of the hardwood component of the OCC were assumed to be close to the semi-chem hardwood. The softwood component was assumed to be similar to a southern pine.

Attributes of the OCC blend was generated by mixing the two streams in a mixer. Attributes of the semi-chem and OCC are summarized in Table 2. All fiber tensiles were initialized to 10 km, fiber modulus to 4.5 GPa, cell wall thickness to 1.2 microns, and specific bond strength to 0.2×10^7 Pa.

Refining of the semi-chemical furnish reduced the fiber length, tensile strength and elastic modulus slightly and the freeness by 15 to 30 ml. The OCC and semi-chemical fiber lines were combined and refined in the tickler refiner. Increased load and consistency in the tickler refiner reduced freeness and average fiber length but had little effect on other attributes. The screening and cleaning system was modelled in detail. However, there was very little net effect on fiber attributes such as fiber length and freeness. Fiber losses from the cleaning system totaled less than one percent of total flows.

The headbox and forming wire were simulated by fourdrinier blocks which determined profiles of the drainage rate, white water consistency, mat basis weight and mat moisture. The important factors in the forming section which influence dry sheet properties are fiber contact area, sidedness, formation, fiber orientation, final freeness and fiber length distribution. The formed sheet freeness and fiber length were similar to the tickler discharge. The lower headbox freeness was more a reflection of white water closure and recycle and had little influence on final sheet properties. However, headbox freeness did influence machine drainage, dry line location, moisture profiles in the press section and the steam consumption to achieve the final 93% dryness.

Formation levels were influenced by fiber length, forming consistency and jet to wire velocity ratio. However, the relatively high basis weight of the corrugating medium reduced the influence of these variations on formation. Formation variations were most important in the handsheets. Variations in jet-to-wire ratio had only a small effect on fiber orientation. The fiber orientation factor, defined as the cotangent of the average fiber orientation angle relative to the machine direction, was adjusted initially to 1.5 and maintained at that value during the test. These observations were substantiated by the accurate prediction of MD/CD tensile and modulus ratios of the machine paper throughout the test and the insensitivity of tensile ratio to trial variables.

Press loading influenced water removal and moisture profiles in the press section and the steam consumption required to reach a fixed 93% sheet dryness. Increased press loading also increased fiber contact area resulting in increased density and sheet strength.

The can dryer section determined the steam consumption required to achieve a target final dryness. In this section hydrogen bonding is significant. All MD stretch due to speed differentials along the machine were assumed to be lumped into the dryer section. The net MD wet stretch was adjusted to 2 % and unchanged during the trial.

A single nip calender was simulated with a calender block. In this block the sheet is densified and the surface roughness, smoothness, gloss and porosity are changed. Densification in the calender increased fiber contact but did not strongly influence bonding. Thus tensile strength, specific modulus or compressive strength were not changed while density and elastic moduli were changed.

Property Models

The effects of papermaking variables can best be interpreted through the paper property models. The Concora (N) is defined in terms of flat crush, FC (kPa),

$$Concora = 235.85 + 9.09\,(FC - 206.7) \qquad (1)$$

where FC is defined in terms of MD STFI

$$FC = 206.7 + 11.5\,(STFI_{MD} - 2.98) \qquad (2)$$

MD and CD STFI (kN/m) and Ring Crush (Kn/m) are defined in terms of sheet thickness, t, mm, and directional elastic moduli.

$$\begin{aligned} RC_{md} &= 0.00435T_1 + 0.00181T_2 - 0.6307 \\ RC_{cd} &= 0.00435T_2 + 0.00181T_3 - 0.6307 \end{aligned} \qquad (3)$$

$$\begin{aligned} STFI_{MD} &= 1.397 + 0.00613T_3 \\ STFI_{CD} &= 0.800 + 0.00613T_2 \end{aligned} \qquad (4)$$

where

$$\begin{aligned} T_1 &= (E_x t)^{3/4}(E_y t)^{1/4} \\ T_2 &= (E_y t)^{3/4}(E_z t)^{1/4} \\ T_3 &= (E_x t)^{3/4}(E_z t)^{1/4} \end{aligned} \qquad (5)$$

The elastic moduli (Gpa) are defined in terms of fiber modulus (Gpa), sheet density (g/cm^3), bond density and interactions between bond density, wet strain and fiber orientation.

$$\begin{aligned} E_x &= \overline{E_f}(0.278+\rho_b^e(7.043\rho_b^e+6.513\Theta+1.9WS)) \\ E_y &= \overline{E_f}(-0.8081+\rho_b^e(16.8-4.6\Theta-0.539WS)) \\ E_z &= \overline{E_f}(0.308+\rho_b^e C) \end{aligned} \qquad (6)$$

where

$$C = -1.25 + 1.44\rho_b^e + 0.011\Theta + 0.029\,WS \qquad (7)$$

Θ, and WS, are the fiber orientation factor and the cumulative percent change in MD stretch respectively and

$$\overline{E_f} = \frac{E_f \rho}{10 \rho_b^e} \qquad (8)$$

ρ and ρ^e_b are the sheet bulk density (g/cm^3) and effective bond density respectively which are functions of the performance attributes of the fibers and the network such as the fiber contact area, bond area, cell wall thickness, fiber stiffness, yield, freeness and formation level.

$$\frac{1}{\rho} = \frac{1}{\rho_u} + \left(\frac{1}{\rho_l} - \frac{1}{\rho_u}\right)\left(\frac{1}{S_b}\right)^2 \qquad (9)$$

where the unbonded density is given by

$$\frac{1}{\rho_u} = 0.764 + 0.00477\,CSF + 0.1146\,CWTS \qquad (10)$$

and the upper limit to sheet density is given by

$$\frac{1}{\rho_l} = \frac{1}{\rho_u} + 43.14 + 0.08726\,Y - 0.5866\,CSF \qquad (11)$$

Y is the percent pulping yield. CSF is the Canadian Standard Freeness, ml. S is the fiber stiffness factor (dimensionless). CWT is the fiber cell wall thickness, microns. The term S_b is the fiber contact function defined later. The bond density is defined by the same function as the sheet density with the bond area function S_a substituted for the fiber contact function. The effective bond density is defined in terms of the bond density, formation factor, F, and the total fraction of suspended solids in the sheet, X_s.

$$\rho_b^e = \rho_b F (1 - X_s) \qquad (12)$$

The elastic properties are then defined in terms of the effective bond density and the bulk density. The specific elastic constants are defined as the dimensional elastic constant divided by bulk density. The specific constants are therefore independent of density and depend only on bonding, fiber modulus and residual strains in the sheet which are accounted for by wet stretch and fiber orientation.

The relationship between the bond area function and the fiber contact function is simply a function of the current moisture level in the sheet given by

$$S_a = S_b e^{-(X_m - 0.075)} \qquad (13)$$

where X_m is the weight fraction moisture in the pulp or sheet and is, therefore, a function of dryer conditions. The fiber contact function actually varies throughout the thickness of the sheet and is tracked specifically on the top and bottom surfaces of the sheet in order to simulate sidedness effects through forming, pressing and calendering. These include differences in smoothness, gloss and opacity.

The fiber contact function depends on the hydrodynamic specific surface of the fibers (i.e. CSF), the conformability of the fibers under the pressure impulse during a pressing step.

$$S_b = S_{bi} + (S_h - S_{bi})(1 - e^{-P_k P}) \qquad \textbf{(14)}$$

P_k is defined to conform to the Han power-law function observed for densification by wet pressing but also to not over-densify through several press nips.

$$\begin{aligned} P_k &= -\frac{\ln(Z)}{60} \\ Z &= 1 - \frac{S_{bi}}{(S_h - S_{bi})} e^{(AP + BP\ln(60))} \\ AP &= 0.4 + 1.27x10^{-4} CSF \\ BP &= 3.0x10^{-3} CSF - 1.5x10^{-4} Y \end{aligned} \qquad \textbf{(15)}$$

P_k is also defined to predict the conditions of a handsheet mold (i.e., lower pressure and longer pressing time) as well as the shorter duration, higher peak pressure impulse of the commercial press nip. The function above relates the inlet or initial value of S_b over each pressing operation. The degree of densification correlates with the dewatering in the nip. The initial unpressed fiber contact function is generated by the forming blocks and is a function of the fiber specific surface and fiber conformability given by

$$S_{bi} = (0.0734 - 0.000654Y)\ S_h \qquad \textbf{(16)}$$

where S_h is the maximum specific surface area of the fibers. The relationship between S_h and CSF in the fiber contact relationship is given by

$$S_h = 95.7 - 0.12\,CSF \qquad \textbf{(17)}$$

The relationship between CSF and hydrodynamic specific surface area is given by

$$CSF = e^{7-0.33A} \qquad \textbf{(18)}$$

A is defined in terms of the fiber length distribution and a refining factor as

$$A = 1 - \sum_{i=1}^{10} X_i \ln\left(\frac{L_i}{2.4}\right) \qquad \textbf{(19)}$$

where X_i and L_i are the weight fraction and average length of the ith fiber and K accounts for differences in surface area development dependent upon the uniformity and extent of refining, species and pulping on external fibrillation (Jones 1989). Additional relationships are defined (but not shown) between the fiber length distribution, surface area per fiber, and S_h. Changes in refining influence fiber length and width distribution, CSF, fiber stiffness factor, and, to a small extent, fiber tensile and modulus. These relations depend on specific power and energy per impact in the refining zone. Mixing causes various types of fibers to be brought together and the resulting mixture characteristics tend to conform to the weight-average of the various streams.

Separations in screening and cleaning in the current system have little effect on the average fiber attributes entering the forming section. However, for dirty furnishes these operations remove shives and dirt thus improving the effective bond density, modulus, and compressive strength.

On the forming wire, fines are selectively removed to the white water while basis weight, fiber contact area, formation, and fiber orientation are built into the sheet. Formation efficiency is defined in terms of the coefficient of variation in mass density so as to range between 0 and 1. The formation factor, F, is a function of forming consistency, CO, average fiber length, L, Schoppler-Riegler slowness, SR, and jet to wire ratio, JWR.

$$\begin{aligned} F &= 0.01 f_1 JWRC \\ f_1 &= 119.65 - 25CO - 27.4L - 0.09SR + 0.23SRL \end{aligned} \tag{20}$$

where SR slowness is defined as

$$SR = \frac{(950 - CSF)}{12.5} \tag{21}$$

The JWRC is equal to 1 unless the following conditions hold,

$$\begin{aligned} JWRC &= \frac{JWR}{0.9} \quad 0 < JWR < 0.9 \\ JWRC &= \frac{1.1}{JWR} \quad JWR > 1.1 \end{aligned} \tag{22}$$

The MD/CD tensile ratio is given by

$$R_{MD/CD} = 0.335 - 0.583WS + 0.708WS\Theta + 0.6345\Theta^2 \tag{23}$$

DATA ANALYSIS

In the data analysis it was assumed that transient process data could be analyzed using a steady-state simulation model with variable inputs.

Measurement Variability

Measurement variance was based on the distribution of the mean for a total of 114 machine paper samples and 120 handsheet samples (10 to 20 replicates per sample). The overall test variance for each machine paper or handsheet property was based on the pooled test average. The pooled data for each reel interval included three CD sets and three rolls per reel. Measurement variances could not be determined on density, basis weight and caliper, which had only a single measurement per sample. Table 3 shows the mean, coefficient of variation, CV, correlation coefficient, and confidence band for each of the machine paper property. The confidence band is the percent measurement variance defined above. The confidence bands for each variable are twice the standard deviation divided by the mean and expressed as a percent.

The correlation coefficient is determined by regression of the predictions against the measurements using a single factor model with no intercept,

$$\textit{Measurment} = \textit{Coefficient} \times \textit{Prediction} \quad (24)$$

All R-squared values exceeded 0.995. The high R-squared values indicated that the models could be corrected to agree closely with the data. The proximity of the correlation coefficient to unity indicates that the corrections are not excessive. Comparing the difference of the correlation coefficient from unity with the corresponding confidence band in Table 3 also indicates that the uncorrected predictions fall within the measurement error. These statistical tests indicate that the models are generally valid for this grade.

Similar conclusions can be drawn from the handsheet data summarized in Table 4. Although both the measurement variance and the model error are larger for the handsheet data, the corrected models predict most of the measurement variations and, except for porosity, the corrections are not excessive.

The zero span tensile of the light weight sheets varied from 6.7 to 12 km with a mean of 9.0 km indicating that the assumed average fiber tensile attribute of 9.5 km (see Table 1) was reasonable.

EFFECTS OF PROCESS VARIABLES ON MACHINE PAPER PROPERTIES

The simultaneous variations in several process conditions made it difficult to obtain meaningful interpretations of the machine or handsheet property transient profiles (property vs. reel number). Therefore, the effects of the process variables were determined made by comparing the mean property values and by statistical regression.

Profiles of caliper, MD modulus, and Concora versus reel number are shown in Figures 1 through 3. Each "X" indicates the average measurement of a roll or set taken for each reel. Aside from the obvious effect of calender stack unloading for reels 7 and 8, the effects of other variables are difficult to discern from the data.

Machine Speed and Calender Load

Table V below shows that neither machine speed nor calender load affected the mean compressive or tensile properties greater than measurement variance. However, density, caliper and elastic moduli were changed significantly by calender loading. Increased density resulted in increased modulus but decreased caliper and unchanged specific modulus. The insensitivity of specific modulus resulted in insensitivity of compressive properties to these variables.

From the models, one might predict that the MD/CD ratio of the sheet could have been affected by the calender stack loading, possibly as a function of stretch or stress relief. However, the measured properties did not support this conclusion.

The sheet property data correlated weakly with the trial variables indicating that the properties were weakly dependent on these process variables. MD tensile correlated with machine speed (33%), calender loading (10%) and sheet density (5%). Burst index correlated with the product of MD and CD tensile (60%) as expected from the property models. Elastic moduli correlated with sheet density (50%). CD ring crush was weakly dependent on machine speed (6%) and concora showed a weak (10%) dependence on calender loading. Sheet density was sensitive to calender loading (40%) and less sensitive to high density CSF and OCC content. Percentages above are the percent of the sum of squared error accounted for by each term. Surprisingly neither the statistical analysis nor visual inspection of the data showed any sensitivity to refiner power or press load. Other statistical comparisons indicated that the effects of machine speed and calender load were also within measurement error.

OCC Content

Although OCC content varied from 18% to 36%, there was a relatively minor affect on compressive properties. The MAPPS models show that the OCC fiber attributes are similar to those of the semi-chemical fibers. Thus the mixture attributes did not change greatly with increasing OCC. Visual inspection of the data indicated that tensile strength and burst were highest near the peak in OCC. The freeness of the mixture did decrease with increasing OCC which increased sheet density, reduced caliper and increased modulus. However, the specific modulus and compressive strength did not change significantly.

MD modulus increased by about 0.9 Gpa, approximately 30%, while CD modulus increased by 0.42 Gpa, approximately 25%. The CD ring crush increased by 0.196 (25%) comparable to the measurement standard deviation discussed below, an insignificant change. Concora changed less than the measurement standard deviation and was not significant at 90% confidence.

The model sensitivity analysis and visual inspection of the data indicated that increasing OCC actually improved tensile, burst and ring crush mainly through decreased CSF and improved bonding. The highest tensile and burst values occurred during the period just after the peak in OCC content from 35% down to 30% while tickler discharge CSF was also relatively high near 450 ml (primary refiner power was 0.19 mJ/kg) and third nip press load was also at its high value of 113.83 Kn/m. A sensitivity analysis with the model showed that the tensile and compressive properties increase slightly with increasing OCC content due primarily to decreasing OCC freeness. The increase in burst index and breaking length is about 10% for the maximum variation in OCC in the test.

Refining and Wet Pressing

High refining power decreased tensile and burst through decreased fiber tensile, increased sidedness and decreased average bond area. Press and calender load had very little effect. The effects of refining and pressing were felt mainly indirectly in the sheet dewatering and steam consumption in the dryer.

CONCLUSIONS

Based on the two validation criteria and estimates of measurement error, the model system was validated for corrugating medium. Calculated correction factors should be applied to some of the property predictions. While the measurements could not be correlated with the test variables by standard methods, they correlated strongly with model predictions with relatively small corrections. Sensitivity analysis with the validated models showed that, contrary to most expectations, OCC content improved tensile strength but had little effect on compressive strength.

Calender load and machine speed had only a minor effect on most properties. Also surprising, statistical analysis showed that both press load and refining power had no effect on properties under these conditions, while sensitivity analysis showed that refining may have had a negative effect on tensile properties. There was some evidence that machine speed affected MD tensile. Tensile and modulus ratios were also insensitive to test variables. There was evidence of transient effects when looking at the handsheet CSF and machine paper data but these effects could not be separated from the overall variations in the data. Future transient simulations may clarify the roll of transient effects.

ACKNOWLEDGEMENTS

The author wishes to thank the member companies of the Institute of Paper Science and Technology and especially those at MacMillan Bloedel, Pinehill, Alabama for their support and assistance in this work.

REFERENCES

1) Jones, G. L., Pulp and Paper Mag. Can., 89(6):T213 and 91(2):T81 (1989).
2) Jones, G. L., Tappi, 72(10):189-197 (1989).
3) Jones, G. L., X. N. Nguyen, Tappi, 73(7):160-168 (1990).
4) Jones, G. L., Tappi, 73(11):113-118 (1990).
5) MAPPS Technical Documentation, The Institute of Paper Science and Technology (1991).
6) Habeger, C. C., W. J. Whitsitt, "A Mathematical Model of Compressive Strength in Paperboard," Fiber Sci. Technol., 19:215-239 (1983).
7) Perkins, R. W. Jr., R. P. McEvoy, "The Mechanics of the Edgewise Compressive Strength of Paper," Tappi, 64(2):99-102 (1981).
8) Wink, W. A., J. A. Watt, W. J. Whitsitt, G. A. Baum, "Role of Fiber Axial Modulus on Compressive Strength," Fiber Sci. Technol., 20:245 (1984).
9) Whitsitt, W. J., "Relationships Between Elastic Properties and End-Use Performance," Project 2695-23, Report One to FKBG of the API, (1985).

Table 1: Test Variables and Data Ranges

Variable	Range	Average	Base Case
OCC content, %	18 - 38	27	18
Primary Refiner Power Mj/kg	0.104 - 0.366	0.204	0.104
Calender Loading	on - off	-----	
Tickler Refiner Power Mj/kg x 1000	3.34 - 20.1	10.0	3.34
Wire Speed, m/s	7.112 and 9.65	---	7.112
Third Nip Pressure, Kn/m	84.1 - 113.8	100.9	84.1

Table 2: High Density Tank PAT Initialization

Attributes	Semi-chem	OCC furnish Hardwood	OCC furnish Softwood	OCC Mixture
Avg. Fiber Length, mm	1.4	1.4	3.0	2.2
Avg. Fiber Width, mm	0.02	0.02	0.04	0.03
Yield, %	74	74	60	67
CSF, ml	656	150	667	316

Table 3: Measures of Model Validity - Machine Paper Properties

Property (114 data sets)	Mean	CV	Corr Coef	Conf Band
MD Tensile, km	6.0	5.98	0.994	13
CD Tensile, km	2.54	7.43	1.01	15
MD Stretch, %	1.64	5.93	0.915	27
MD/CD ratio - modulus - tensile	 2.36 2.35	 7.18 4.78	 0.995 0.998	 -- --
Burst Index	2.90	7.22	0.957	16
MD Modulus, Gpa	4.33	4.59	0.948	14.3
CD Modulus, Gpa	1.85	8.60	0.871	12
Caliper, mm	0.2113	5.0	1.031	--
Concora, N	238.5	5.06	0.92	13.2
CD Ring Crush	0.95	18.4	1.45	39.4
CD STFI	2.54	4.59	1.173	44
Gurley Porosity	20.48	20.6	0.974	--

Table 4 Handsheet Data (120 data sets)

Property	Mean	CV	Coeff-icient	Confidence Band %	R-Squared
CSF, ml	503	12.8	1.07	--	0.984
Tensile, km	3.64	20.9	0.936	12	0.959
Concora, N	242.5	19.4	0.766	13	0.964
Ring Crush	1.56	25.1	1.62	12	0.939
Burst Index	2.30	18.1	1.01	20	0.968
Porosity	16.0	75.2	1.03	38	0.647
Density	0.41	9.1	0.982	--	0.992

Table 5: Effect of Calender Load and Machine Speed

Property	Calender on	Calender off	Machine Speed m/s 7.11	Machine Speed m/s 9.65
Modulus				
MD	4.40	3.52	4.39	4.30
CD	1.88	1.46	1.90	1.82
MD/CD	2.35	2.35	2.35	2.35
Tensile	5.81	5.97	5.72	6.08
Burst Index	2.90	2.88	2.79	2.96
Density	0.60	0.52	0.595	0.59
Caliper	0.209	0.245	0.206	0.214
Concora	223.4	239.8	242.8	236.4
CD STFI	2.54	2.56	2.56	2.50
CD Ring Crush	0.97	0.77	0.92	1.02

Machine Paper Caliper

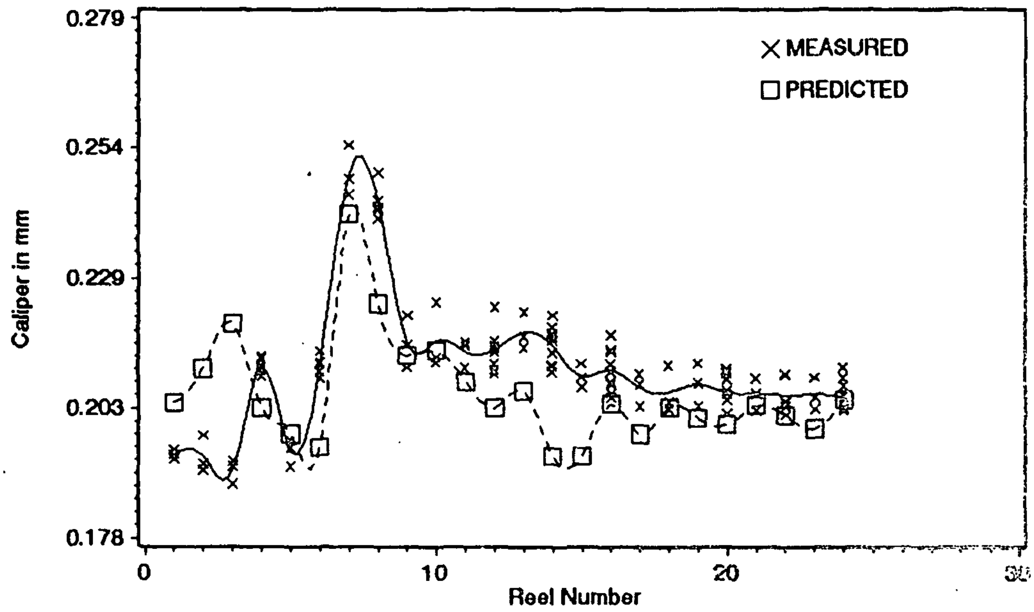

Figure 1

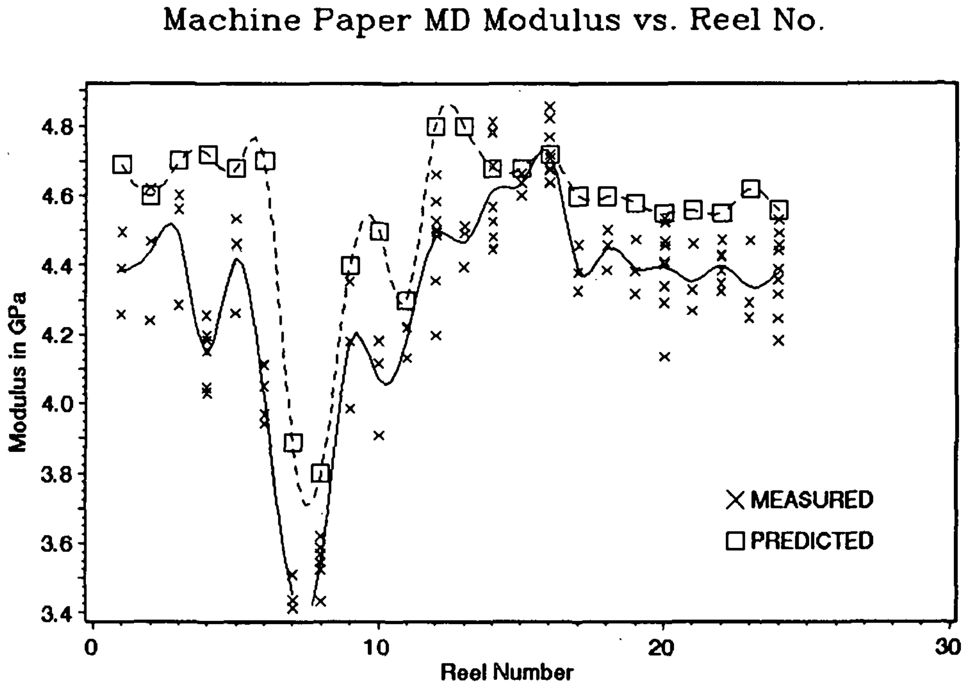
Machine Paper MD Modulus vs. Reel No.
Modulus in GPa
Reel Number
MEASURED
PREDICTED
4.8
4.6
4.4
4.2
4.0
3.8
3.6
3.4
0
10
20
30

Figure 2

Machine Paper Concora vs. Reel No.

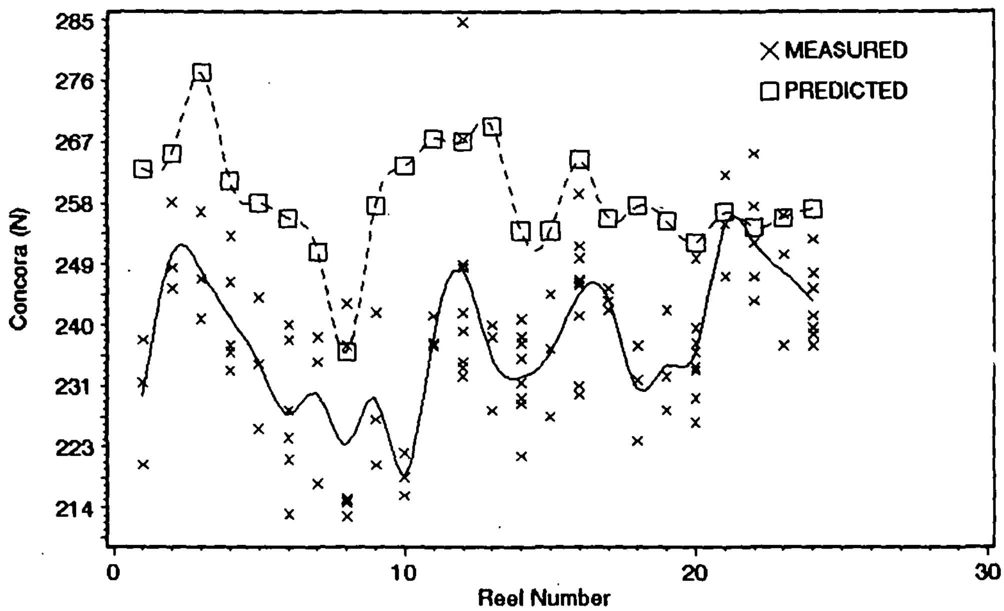

Figure 3